An Automatic Tunnel Shotcrete Robot

Xuebin Lin
School of Automation
Central South University
Changsha, China
100400880@qq.com

Di Song
School of Automation
Central South University
Changsha, China
980902922@qq.com

Mi Qin
School of Automation
Central South University
Changsha, China
460269512@qq.com

Wenting Zhang
School of Automation
Central South University
Changsha, China
790187687@qq.com

Xiaoyu He
School of Automation
Central South University
Changsha, China
hexiaoyu@csu.edu.cn

Bin Xie*
School of Automation
Central South University
Changsha, China
xiebin@csu.edu.cn

***Abstract*—At present, tunnel shotcrete construction in tunnel support is mainly carried out by manual control of multi-DOF (Degree of Freedom) shotcrete machine. Due to the harsh environment of the tunnel and the high labor intensity, the work is extremely harmful to the tunnel construction workers. In order to improve the automation level of the tunnel construction industry, this paper designed a fully automatic tunnel shotcrete robot based on the 8-DOF shotcrete machine. The research in this paper mainly includes four parts: kinematics modeling, environment perception, trajectory planning and trajectory tracking control. We carried out the control precision experiment and motion tracking experiment under the simulated tunnel. It shows that the automatic shotcrete robot designed in this paper basically meets the requirements of actual tunnel construction.**

Keywords—shotcrete robot, kinematics modeling, environment perception, trajectory planning.

I. INTRODUCTION

The tunnel initial shotcrete refers to the first layer of the tunnel surface, which makes the surface of the tunnel smoother and regular. There are various supporting in initial shotcrete, such as arches and protective nets. Due to the complexity of the working conditions, the initial shotcrete is basically controlled by the manual control of the shotcrete machine [1]. During the construction process, the high-density dust is extremely harmful to the construction workers. In addition, the high-intensity labor and the requirements of high technical proficiency lead to the difficulty in recruiting the operator and even the labor shortage.

Since there is little research on the automatic shotcrete robot and no mass-produced automatic shotcrete robot in the world, it will be explained according to the main research contents it contains in this paper.

At present, few studies were carried out on the inverse kinematics of redundant manipulators. Whitney [2] obtains the inverse kinematics solution of Redundant Manipulators by minimum norm method, and Zhang [3] obtains it by particle swarm optimization. However, the above methods are difficult to meet the real-time requirements of industry, and they are generally only used for off-line computing. M. Shimizu [4] use a parametric approach to the SRS robotic arm, but this method is unsuitable to our object due to the mechanical structure limitation.

Fig. 1. KC series shotcrete robot (8-DOF).

Iterms of 3D reconstruction technology, low-cost sensors with high-quality 3D environmental information have received greater attention in recent years [5]. For the design and use of sensors, Anindya Harchowdhury [6] proposed a low-cost 3D sensor that uses a high-speed servo system to point-control the lidar to generate 3D perception of the surrounding environment. Suitable parameters for 3D laser scanning can obtain high quality tunnel point clouds [7], and TLS(Terrestial Laser Scanner) system simulate the error of the measured point cloud [8]. The detection of tunnel crack width and depth can be achieved by a semi-supervised computer vision system [9]. Lai P [10] proposed a new mesh deformation algorithm, which can obtain a very intuitive mine roadway rasterization effect. It proposed a new idea for the indexing of tunnel-like cylindrical irregular surface point clouds.

In terms of spray trajectory planning, Suh S H [11] developed an off-line programming system that integrates software and hardware to solve the problem of automatic spraying. In order to solve the problem that industrial automation spraying is limited to large-volume robots, Andreas Pichler et al. [12] proposed the use of range image data to obtain the geometry of an unknown object and the method of automatically generating robotic paint trajectories. With the improvement of computer capabilities, Ming J. Tsai used machine vision technology for path planning [13].

Corresponding Author: Bin Xie, e-mail: xiebin@csu.edu.cn.

Funding Agency: Changsha Keda Intelligent Equipment Co., Ltd.

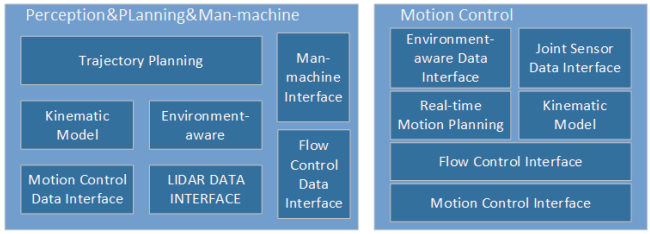

Fig. 2. Software system module division.

In order to fill the gap in automatic tunnel shotcret, a new automatic shotcrete robot was designed to get rid of the dependence on the operator and realize the unmanned tunnel shotcreting in this paper.

The structure of this paper is organized as follows. The second part will elaborate on the important components of the automatic shotcrete robot. The third part shows and analyzes the test results of the automatic shotcrete robot. The last part makes conclusions.

II. THE SYSTEM DESIGN

A. Automatic shotcrete robot overview

Our goal is to achieve the automatic tunnel shotcrete of the specified model shotcrete machine as shown in Fig. 1, and to form a complete intelligent control system. The automatic tunnel shotcrete covers three main technical contents: shotcrete robot modeling, modeling and identification of tunnel surface, trajectory planning and trajectory tracking control.

In order to achieve our goal, hardware and software both need to be considered.

1) Software design

The software system as shown in Fig. 2 is mainly for real-time motion control and rapid environment-aware. The former controls the robot arm to realize the specified action in real time through the joint sensor data and the trajectory planning result. The latter receives environment-aware data to acquire the tunnel situation and output planning results quickly.

2) Hardware design

The Hardware system is shown in Fig. 3. The core operation unit is composed of a motion controller and a IPC(Industrial Persional Computer). The former provides real-time control operation and output capability, while the latter provides strong computing capability. The sensor usage of each joint are shown in Table I. The angle measurement of the 5th joint is calculated by the elongation of the cylinder due to the mechanical structure limitation.

B. Kinematics modeling

Robot kinematics modeling is the basis of trajectory planning and control, including forward kinematics and reverse kinematics.

Considering that the object is an 8-DOF machine which contains two kinds of joints, respectively rotation and Translation, we chose the coordinate system movement for the forward kinematics model, instead of traditional D-H (Denavit-Hartenberg) method. The base coordinate system is established on the base of the manipulator, then the coordinate system is translated and moved to the center of the next joint. If the next joint is a translation joint, the coordinate system continues to be translated. If the next joint is a rotary joint, the coordinate system continues to be rotated.

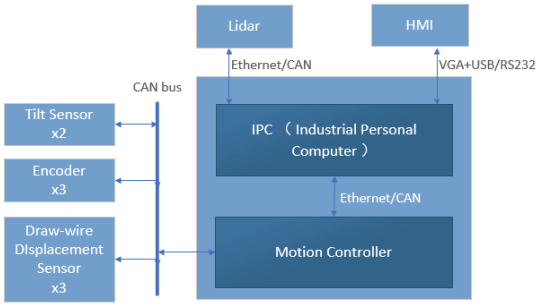

Fig 3. Hardware system framework.

TABLE I. SENSOR PARAMETERS REQUIREMENTS AND USAGE

Joint	Joint Type	Range	Precision	Sensor Type
1	Rotary Joint	360°	0.1°	Encoder
2	Rotary Joint	180°	0.1°	Tilt Sensor
3	Translational Joint	3000mm	1mm	Displacement Sensor
4	Rotary Joint	180°	0.1°	Tilt Sensor
5	Rotary Joint	360°	0.1°	Displacement Sensor
6	Translational Joint	2000mm	1mm	Displacement Sensor
7	Rotary Joint	360°	0.1°	Encoder
8	Rotary Joint	240°	0.1°	Encoder

This paper obtained the solution of the inverse kinematics model by the Fixed-Joint-Angle method [14] and the Pose Separation method. Combined with the structure of the manipulator, the Monte Carlo method is used to draw the reachable point cloud image of the end effector under different fixed joints. Considering the requirement of the end space in construction, the fifth joint and sixth joint were selected as parametric joints. Then the analytical solutions of the remaining six joints were solved according to the results of the Forward-Kinematics model.

For the inverse kinematics model, the first step is to obtain the position and orientation of the end. At this time, the transformation matrix of the end coordinate system relative to the base coordinate system is known, and is set to

$$R = \begin{pmatrix} r_{11} & r_{12} & r_{13} & p_x \\ r_{21} & r_{22} & r_{23} & p_y \\ r_{13} & r_{23} & r_{33} & p_z \\ 0 & 0 & 0 & 1 \end{pmatrix}. \quad (1)$$

And

$$R = T = A_1 \bullet A_2 \bullet A_3 \bullet A_4 \bullet A_5 \bullet A_6 . \quad (2)$$

Because the transformation matrix of first joint relative to the base coordinate system is

$$R = \begin{pmatrix} C\theta_1 & S\theta_1 & 0 & 0 \\ -S\theta_1 & C\theta_1 & 0 & 0 \\ 0 & 0 & 1 & 0 \\ 0 & 0 & 0 & 1 \end{pmatrix}. \quad (3)$$

Then both sides of equation (2) is multiplied by A_1^{-1} as equation (4).

$$A_1^{-1} \bullet R = A_2 \bullet A_3 \bullet A_4 \bullet A_5 \bullet A_6 . \quad (4)$$

Based on equation (4), multiple equations can be established according to the elements of the corresponding positions of the left and right matrices. If the left multiplication A_1^{-1} is still difficult to solve, the current formula continue to multiply both sides by A_2^{-1}, until the listed equations can solve the analytical solution of each joint. The inverse solution of the first joint is obtained as follows.

$$\theta_1 = \arcsin\left(\frac{a_1}{\sqrt{A^2 + B^2}}\right) - \arctan\left(\frac{B}{A}\right). \quad (5)$$

With

$$\begin{aligned} A &= (a_2 + a_3) \bullet r_{13} - p_x + a_3 \bullet r_{12} + a_4 \bullet r_{11}, \\ B &= -p_y + (a_2 + a_3) \bullet r_{23} + a_5 + a_4 \bullet r_{12} \end{aligned} . \quad (6)$$

$a_i (i = 1,2,3,4,5)$ are known mechanical arm structural parameters.

According to the analytical solution of the first joint, the analytical solution of the rest joint could be obtained in turn. Based on the criterion of reducing the mobility and avoiding the joint limit, the optimal solution was selected from 16 sets of inverse solutions to control the manipulator, and it was verified with the forward kinematics model .

C. 3D reconstruction

After completing the kinematics modeling of the shotcrete robot, it is necessary to model and identify the tunnel surface, and obtain the characteristic information through the 3D reconstruction technology as the basic data of the shotcrete planning.

1) 3D reconstruction system design

According to the operation mode and working environment of the shotcrete machine, the scanning equipment was mounted on the arm of shotcrete machine to follow the arms movement so as to reducing obstacle obstruction and increasing the scanning range. Therefore, the scanning device is required to have small volume, light weight, dust resistance, high precision, low cost and high protection level.

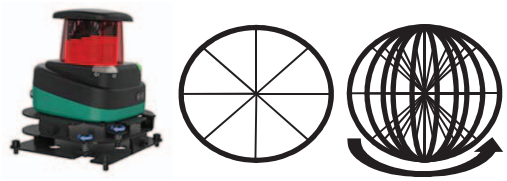

(a) (b) (c)

Fig 4. (a) 2D single-line lidar; (b) schematic diagram of the operation of a 2D single-line lidar;(c) working diagram after combining the electronically controlled pan/tilt.

Fig 5. Scanning device installation.

3D reconstruction usually uses equipments such as binocular stereo camera, total station or laser scanner. The binocular stereo camera is low in cost, but it requires a sufficient light source and a clean environment. It is susceptible to occlusion and noise when used in tunnel filled with dust. The total station is not suitable for collecting high-density point cloud information. And the need for fixed-position reflectors is inconvenient for use in construction tunnels. Laser scanners include 2D and 3D scanners that overcome most environmental factors, where existing 3D scanners are expensive and bulky .So they are not suitable for shotcrete robot.

Therefore, this paper presents a 3D scanning device that controls the 2D lidar rotation scanning by electronically controlled pan/tilt. This device meets the basic requirements of the equipment in this paper. It can cooperate with the shotcrete machine to complete the data acquisition and analysis of the construction area.

Considering that the scanning process requires a wide field of view, we installed the scanning device on the front end of the 6th joint of the body, and converted the coordinate system of the lidar to the coordinate system of the body through forward kinematics. In order to ensure the accuracy of data acquisition.

2) Tunnel 3D reconstruction technology

a) Point cloud uniform sampling

The lidar imaging selected in this paper has the following characteristics: the point cloud density is large, and the original data point is about 4 million; the point cloud density is uneven, and the lidar near the point cloud is more dense. In order to homogenize the point cloud, the voxel filtering is first used to downsample, and the downsampled data of about 1 million points is obtained.

b) Extract tunnel point cloud body

Cluster analysis of 3D point cloud was performed by using Euclidean clustering segmentation to realize point cloud segme-

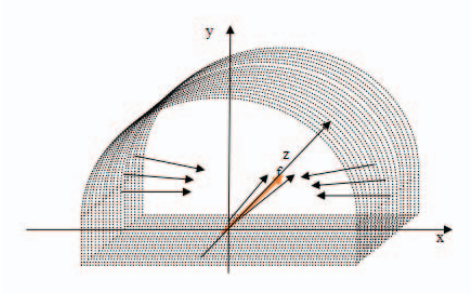

Fig 6. Pairing the joint outer product to find the central axis of the tunnel.

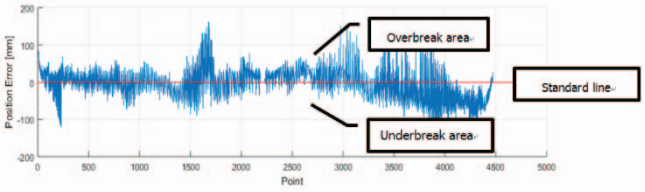

Fig 7. Tunnel slice and standard line alignment results.

ntation. The point cloud that belongs to the tunnel surface should be the largest part after segmentation, and the interference data of walking construction workers and parked vehicles were eliminated. Extract the data belonging to the tunnel surface in the point cloud.

c) Extracting the central axis of the tunnel

The tunnel has a shape feature similar to a cylinder. Based on this geometric feature of the tunnel, the vertical line of the point cloud normal vector could be calculated to obtain the axial direction as shown in Fig. 6. The central axis of the tunnel was represented by an anchor point plus a direction vector, and the coordinates of the anchor point are

$$o(x_0, y_0, z_0) = \sum_{i=1}^{n} (x_i, y_i, z_i) / n \,. \tag{7}$$

The normal vector was translated to the center point of the tunnel and unitized to form a cluster of data points. Planar least squares fitting of these point sets could be used to obtain the plane equation

$$aX + bY + cZ = 0 \,. \tag{8}$$

with

$$\begin{aligned} X &= \{x_1, x_2, \ldots x_n\}^T \,, \\ Y &= \{y_1, y_2, \ldots y_n\}^T \,, \,. \\ Z &= \{z_1, z_2, \ldots z_n\}^T \end{aligned} \tag{9}$$

The normal vector of this plane was taken as the initial calculation result of the direction of the central axis.

After the central axis was determined, the point cloud was uniformly oriented along the central axis, and the actual contour of the tunnel was compared with the standard contour on each of the cut planes so as to obtain the distribution of the overbreak and underbreak and the distribution of the supporting structure as shown in Fig. 7.

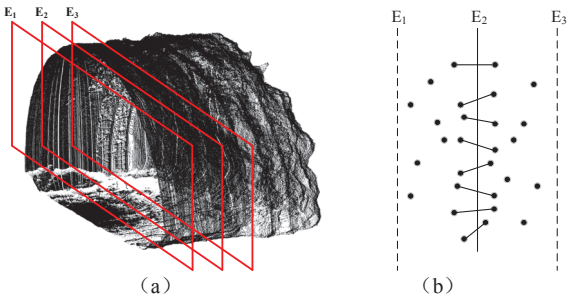

Fig 8. (a) Schematic diagram of tunnel point cloud; (b) schematic diagram of intersection between cutting plane and point cloud.

The tunnel surface over-under-excavation and the distribution of the supporting structure were fed back to the upper monitor, so that the upper monitor could make corresponding motion planning and control the mechanical arm to carry out construction activities.

1) Shotcrete Path Planning

For the 3D point cloud model of the tunnel, the whole tunnel was divided into several sub-areas and each sub-area was smaller than the single shotcrete area of the sprayer.

The moving direction of the sprayer was judged by the 3D point cloud model of the tunnel and the slice thickness was set according to the concrete spray diameter of the sprayer. Then the 3D point cloud model of the tunnel was cut through a series of parallel planes to obtain multi-segment point cloud data. Each adjacent two point cloud data was a group. As shown in the fig. 8 a, E1, E2, and E3 are parallel cutting planes, and two small pieces of point cloud data are obtained.

The closest two points of each group were the matching point pairs, and lines connecting the matching point pairs intersected the cutting plane at a plurality of points. As shown in Fig. 8 b, the intersection of the cutting plane E2 and the line connecting the matching points is the tunnel surface to be sprayed. The surface normal vector of the tunnel surface to be sprayed is extracted by means of plane fitting, and the points to be sprayed are offset by 1m along the inner side of the surface normal vector. After connecting the points, the sprayer path is obtained, and the sprayer orientation is kept parallel to the outer side of the surface normal vector.

B. Motion Control

1) underlying control

The underlying control is the basis of the entire motion control, and the goal is to achieve the control accuracy of all joints in the requirements of kinematic modeling combined. The control is based on the position control of the dynamic PID method, and the control parameter of each joint is adaptively adjusted. The control error of the rotary joint is less than 0.1°, and the control error of the translational joint is less than 1 mm.

2) Motion Tracking Control

According to the target trajectory data given by the trajectory planning and the driving characteristics of the sprayer (hydraulic drive), a multi-joint coupling control algorithm based on single joint dynamic PID control is designed as shown in Fig. 9. After the initialization is completed, it is determined whether the target trajectory data given by the trajectory planning is obtained. Then

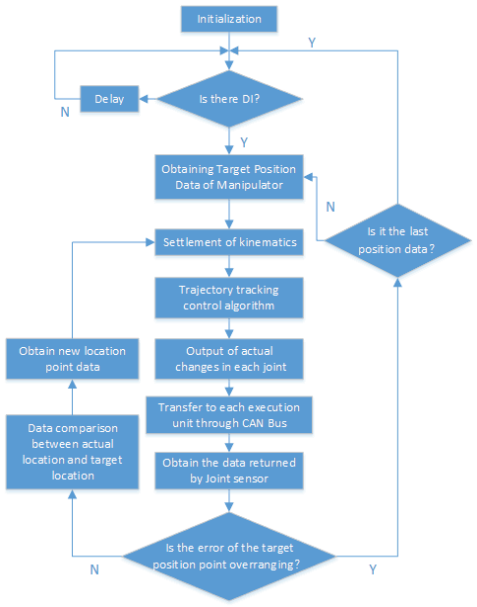

Fig 9. Control algorithm flow chart.

(a) (b)

Fig 10. (a) Fig Simulated tunnel;(b) Robot parking position.

the kinematic model is used to calculate the joint data of each state, and the data is transmitted to the multi-joint coupling control algorithm based on the dynamic PID. The control amount is transmitted to each execution joint, and the control amount is adaptively adjusted with the real-time sensor data.The effect of the algorithm is that the position error is controlled within an ideal range.

The linkage control of each joint with constant load is necessary. The calculation of the load is based on the weight of the sprayed material about 181Kg in the shotcrete pipeline during construction. The maximum value of the position error of the sprayer can be obtained by forward kinematic, which is 10 mm in the X direction, 140 mm in the Y direction and 70 mm in the Z direction, and the position error of each direction allowed during construction is about 150 mm. There are two main reasons for the different errors in the different directions of the sprayer. One is that the control precision of each joint is different where the accuracy of the telescopic joint is relatively higher than the accuracy of the rotating joint, and the other is the error caused by mechanical structure itself such as the weight of the arm causes a large error in the Z direction. The maximum orientation error of the sprayer is about 4.5°, and the angle requirement of the sprayer toward the construction surface is 90°±5°. The accuracy of position and orientation achieved by the trajectory tracking control meet the actual requirements of the shotcrete robot construction.

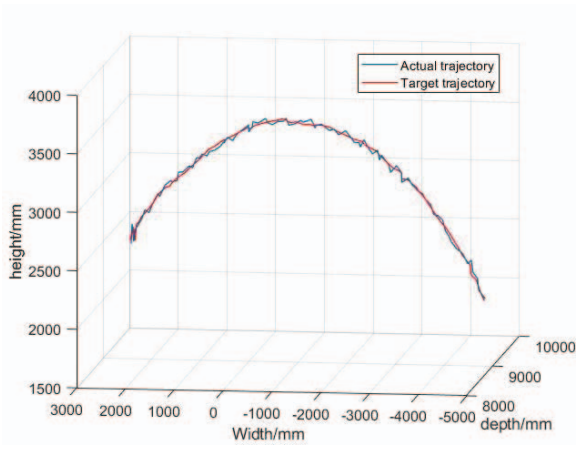

(a)

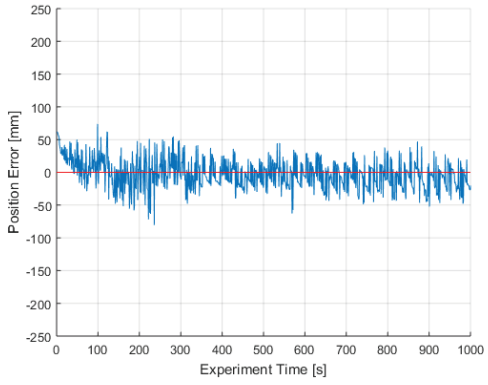

(b)

Fig 11. (a) Comparison of actual trajectory(blue) and target trajectory(red); (b) position error of actual trajectory and target trajectory.

(a) (b) (c)

(d) (e) (f)

Fig 12. (a) Lower left position of the tunnel; (b) lower right position of the tunnel; (c) middle position of the tunnel; (d) right position of steel arch;(e) middle position between steel arches;(f) left position of steel arch.

II. EXPERIMENT

A. Simulated tunnel experiment

The experimental process is as follows: At first, place the shotcrete robot in the built simulated tunnel and restore all joints to the initial position as shown in Fig. 10. Secondly, start the 3D modeling to identify the simulated tunnel information. Thirdly,

the trajectory planning obtains the arc trajectory data of the sprayer movement along the tunnel surface based on the 3D scanning result. Then, the joint sequences is obtained by inverse kinematics and transmitted to the underlying control part. Finally, the control unit controls the shotcrete robot to completes the specified trajectory movement in the simulated tunnel.

B. Experimental analysis

The actual motion trajectory of the sprayer is obtained by the kinematics model, and compared with the trajectory planning as shown in Fig. 11 a, and the position error of the sprayer is as shown in Fig. 11 b. The position error of the sprayer is generally within 100 mm, and the average error is about 50 mm. When simulating a special position in the tunnel, the distance and orientation of the sprayer relative to the wall basically meets the actual shotcrete situation as shown in Fig. 12.

In summary, the fully automatic tunnel shotcrete robot basically meets the actual shotcrete requirements and has certain academic and social significance.

III. CONCLUSION AND FUTURE WORK

This paper describes a fully automatic tunnel shotcrete robot that can be applied to complex tunnels, which can solve the problem of heavy dependence of tunnel construction on the operator and improve the efficiency of tunnel construction. The automatic shotcrete robot mainly includes the kinematics modeling of the shotcrete machine, the modeling and feature recognition of the tunnel surface, and the trajectory planning and motion tracking. At present, the shotcrete robot is in the stage of simulated tunnel experiment. The experimental results show that the performance of the automatic shotcrete robot in the simulated tunnel basically proves the feasibility of the shotcrete robot to complete the tunnel construction task. The next task is to carry out further experiments and improve the technical methods, and realize the automatic construction of the actual tunnel finally.

REFERENCES

[1] Garshol K F, Zieqler C. Computer controlled application of shotcrete: A status report[C]//10th International Conference on Shotcrete for Underground Support. Whistler, BC, Canada, 2006:368−378.

[2] Whitney D E. Resolved Motion Rate Control of Manipulators and Human Protheses [J].IEEE Transactions on Man-Machine Systems, 2007, 10(2):47-53.

[3] Zhang P, Mu X, Ma Z, et al. A PSGO-based method for inverse kinematics analysis of serial dangerous articles disposal manipulator [J]. Information Japan, 2011, 15(12):979-982.

[4] M. Shimizu, H. Kakuya, W. Yoon, K. Kitagaki and K. Kosuge, "Analytical Inverse Kinematic Computation for 7-DOF Redundant Manipulators With Joint Limits and Its Application to Redundancy Resolution," in IEEE Transactions on Robotics, vol. 24, no. 5, pp. 1131-1142, Oct. 2008.

[5] M. Bosse, R. Zlot, and P. Flick. Zebedee: Design of a spring-mounted 3-D range sensor with application to mobile mapping [J]. IEEE Transactions on Robotics vol. 28, no. 5, pp. 1104-1119, Oct. 2012

[6] Anindya Harchowdhury, Lindsay Kleeman, Leena Vachhani. Coordinated Nodding of a Two-Dimensional Lidar for Dense Three-Dimensional Range Measurements [J]. IEEE Robotics and Automation Letters, 2018, 3(4): 4108 – 4115.

[7] Delaloye D, Diederichs M S, Walton G, et al. Sensitivity Testing of the Newly Developed Elliptical Fitting Method for the Measurement of Convergence in Tunnels and Shafts[J].Rock Mechanics & Rock Engineering, 2015, 48(2):651-667.

[8] Roca-PardiAs J, Argüelles-Fraga, Ramón, de Asís López, Francisco, et al. Analysis of the influence of range and angle of incidence of terrestrial laser scanning measurements on tunnel inspection [J]. Tunnelling and Underground Space Technology, 2014, 43:133-139.

[9] Menendez E, Victores J G, Montero R, et al. Tunnel structural inspection and assessment using an autonomous robotic system [J]. Automation in Construction, 2018, 87:117-126.

[10] Lai P, Samson C. Applications of mesh parameterization and deformation for unwrapping 3D images of rock tunnels [J]. Tunnelling and Underground Space Technology, 2016, 58:109-119.

[11] Suh S H, Woo I K Noh S K. Development of an automatic trajectory planning system (ATPS) for spray painting robots[C]. Proceedings of the IEEE International Conference on Robotics and Automation.1991.1948-1955.

[12] Pichler A, Vincze M, Andersen H, et al. A Method for Automatic Spray Painting ofUnknown Parts[C]//Robotics and Automation, 2002. Proceedings. ICRA'02. IEEE International Conference on. IEEE, 2002, 1: 444-449.

[13] Tsai M J, Lee H W, Ann N J. Machine Vision Based Path Planning for A Robotic Golf Club Head Welding System[J]. Robotics and Computer Integrated Manufacturing, 2011, 27(4): 843-849.

[14] Crane C D, Duffy J, Carnahan T. A kinematic analysis of the Space Station Remote Manipulator System [J]. Journal of Robotic Systems, 1991, 8(5):637-658.